Biophysical Chemistry, 49 (1994) 1–12
Elsevier Science B.V., Amsterdam

BIOCHE 01822

Measuring the elastic parameters for inverse bicontinuous cubic phases

R.H. Templer *, J.M. Seddon and N.A. Warrender
The Department of Chemistry, Imperial College, London SW7 2AY (UK)

(Received 28 June 1993; accepted in revised form 30 September 1993)

Abstract

A second-order curvature elastic energy description for the inverse bicontinuous cubic phases has been developed from existing theories. Using this model it is possible to determine curvature elastic parameters from X-ray diffraction measurements on these phases, and we present a preliminary analysis of data from a 2:1 (mol:mol) mixture of lauric acid and dilauroylphosphatidylcholine. A curvature elastic free energy model developed by Turner and co-workers uses as a starting point the same physical principles as the model presented here, but the equations are developed in a very different manner. By re-analysing some of Turner's data using our model we have found a discrepancy between the models, which at present remains unexplained. It has been shown by others that the curvature elastic parameters are related to the variation in lateral stress through the bilayer by three integrals involving the first and second moments of the stress profile and its first derivative with respect to mean curvature. It is our long term aim to measure the stress profile from curvature elasticity determinations. We show that the elastic parameters will only give rise to values which relate directly to the lateral stress profile when the cubic phase is sufficiently swollen, since otherwise the elastic approximations become inaccurate and transverse forces may make significant contributions to the total free energy. A set of diagnostic measurements is suggested which indicates whether or not the cubic phase is sufficiently swollen for the approximations to hold. Using these it seems clear that so far no data have been published in which the cubic phase is sufficently swollen. However, we show measurements which indicate that such systems do exist.

Keywords: Lyotropic liquid crystals; Curvature elasticity; Bicontinuous cubic phases; Lateral stress profile

1. Introduction

The fundamental difficulty in correctly determining the physical effects which control the behaviour of inverse lyotropic liquid crystalline phases is that, in general, the various interactions are of comparable magnitude and are difficult to decouple from each other [1]. We are particularly interested in determining the local intermolecular interactions which lead to inverse mesophases with curved interfaces. This is both interesting in itself, and may have significant implications for understanding the functional control of biological membranes [2].

In this report we will deal exclusively with a discussion of how curvature elastic measurements of the inverse bicontinuous cubic phases might be

---

* Corresponding author.

SSDI 0301-4622(93)E0076-H

made and how these measurements might eventually be used to determine the form of the local interactions, or lateral stress profile. Indeed we will argue that only measurements of the free energy in highly swollen bicontinuous cubic phases allow one to be confident that one is measuring the curvature elastic energy of such mesophases in isolation from all other interactions. This is of course critical if such measurements are to provide a faithful data set for the reconstruction of the lateral stress profile.

The origin of the local intermolecular forces that drive amphiphile/water systems to phases with curved interfaces will be discussed in section 2. The connection between the lateral stress profile and the amphiphilic film's curvature elasticity as derived first by Helfrich [3] and subsequently expanded by Szleifer and co-workers [4], is also described.

In section 3 we present a set of mathematical relationships for the curvature elastic energy of the inverse bicontinuous cubics and the structure of these phases. The mathematical model is a synthesis of the work of various authors who have dealt with aspects of the structure and energetics of the bicontinuous cubic phases [3–8]. As far as we are aware the expressions we will present, although embedded in the published literature, have not been derived in this way elsewhere. This is not to say that we are presenting a fundamentally new physical model of curvature elasticity in these phases, but we have found that the purely algebraic expressions derived here have made it easier for us to understand and model the phase stability and behaviour of the bicontinuous cubics. The results of our work on cubic phase stability will be presented elsewhere.

Turner et al. [9] have published a set of mathematical expressions for analyzing experimental data from bicontinuous cubic phases, which derive from the same physical model of curvature elasticity as our derivation, and can be used to determine curvature elastic parameters. Ström and Anderson [10] have analyzed data on inverse bicontinuous cubics using two approaches, both of which have a very strong geometric flavour. This gives a good deal of insight into the behaviour of their system, but does not give rise to the determination of the elastic parameters which might be used to determine the lateral stress profile.

Rather few measurements of elastic parameters have been made on bicontinuous cubics [9,11] and both have used Turner's model. In section 4 we present a preliminary determination of elastic parameters from our own data on a fatty acid/lecithin mixture and make a comparison between our model and Turner's. The analysis is rather crude and we go on to show how the osmotic stress technique might be used to determine the elastic parameters more accurately. This technique has already been used with success by Chung and Caffrey [11]. However, it is unclear whether measurements of this sort do not include contributions from other energetic terms. We will describe some diagnostic measurements which can be made, that indicate whether or not the cubic phase is sufficiently swollen to make the model valid.

We close in a more speculative vein, by describing in section 5 how data of this sort might be used to determine the lateral stress profile.

2. The origins of curvature elasticity

We can qualitatively understand the desire for curvature in amphiphilic bilayers if we look at the variation in the lateral stress as a function of depth through a bilayer in the L_α phase, fig. 1 (lateral is taken to mean parallel to the bilayer plane). In the chain region the collisions between the fluid chains produces a net positive pressure (taken to correspond to a negative stress). At the polar–apolar interface there is a positive stress, since amphiphiles must pack together as closely as possible in order to reduce aqueous contact with hydrophobic moieties. In the headgroup region the situation is more complex. In the case of headgroups which cannot directly hydrogen bond to each other we can anticipate that at small molecular separations negative stress due to steric and hydration repulsions will occur. As the molecular separation is increased we would anticipate that this stress would fall to zero. Positive stresses could even be obtained in the headgroup region, if residual direct hydrogen bonding between headgroups is present.

Although the integrated lateral stress must be zero, the distribution of stresses will generally give rise to a net bending moment for each monolayer. Where the lipid molecules on either side of the bilayer are the same, as they are in the systems we will consider, the torque on each monolayer is equal and opposite. This means that each monolayer is completely curvature frustrated unless a phase change to a mesophase having curved interfaces occurs [12].

At present only the local lateral interactions in the chain region have been rigorously modelled by theory [4]. It is unclear how accurately the stress at the polar-apolar interface can be modelled, and it is unlikely that the complexities of the behaviour in the headgroup region will be theoretically tractable from ab initio calculations. Given these difficulties we will simplify the problem of the bilayer stress profile by using the ideas first proposed by Helfrich [3,5], in which the bilayer is collapsed into an infinitely thin sheet located at the bilayer mid-plane, fig. 2. The complexities of the lateral stress profile are then subsumed into a sequence of curvature elastic parameters, which are related to the stress profile via three integrals.

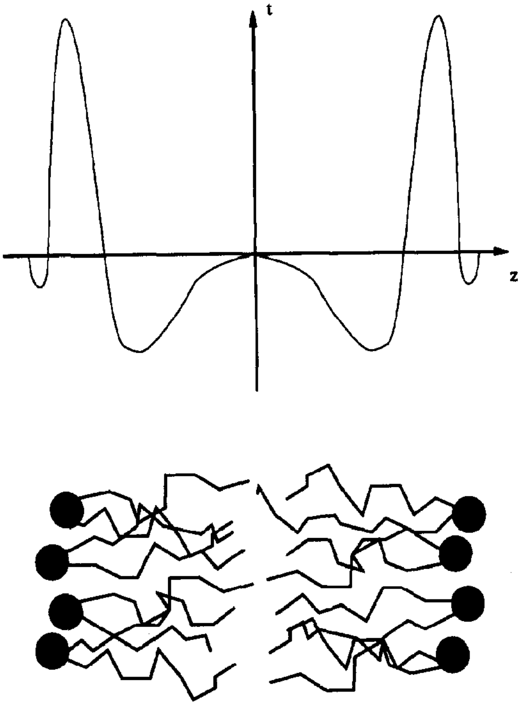

Fig. 1. The lateral stress profile. The lateral stress, t, is shown as a function of depth through a hypothetical bilayer, with the bilayer sketched below. The broad negative stress region arises from chain-chain interactions, the positive stress peak is due to the interfacial tension and the negative blip in the stress is due to repulsive headgroup-headgroup interactions.

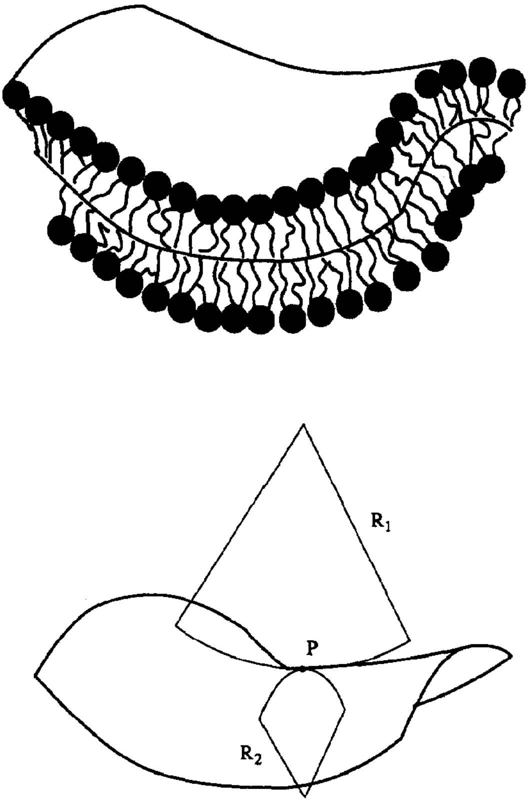

Fig. 2. Modelling the bilayer. The bilayer is modelled as an elastic sheet located at the bilayer mid-plane. The sheet has measurable curvatures $C_1 = 1/R_1$ and $C_2 = 1/R_2$ at all points P on its surface.

The curvature elastic energy per unit area, g_c, can be expressed as an expansion in even orders of the curvatures, C_1 and C_2, fig. 2. For small curvatures we obtain the simplest possible expansion

$$g_c = 2\kappa^b(H - H_0)^2 + \kappa_G^b K, \qquad (1)$$

where H is the mean curvature ($H = \frac{1}{2}(C_1 + C_2)$), K is the Gaussian curvature ($K = C_1C_2$), H_0 is the spontaneous mean curvature, κ^b is the mean curvature modulus for the bilayer and κ_G^b is the bilayer's Gaussian curvature modulus. The spontaneous mean curvature is that mean curvature the system would wish to adopt in the absence of any external constraints and κ^b tells us what energetic cost there would be for deviations away from this. The curvature elastic parameters for the sheet are related to the lateral stress, $t(z)$, of the actual bilayer by the following integrals

$$\kappa^b H_0 = -\tfrac{1}{2}\int_{-l}^{l} t(z) z \, \mathrm{d}z, \tag{2a}$$

$$\kappa^b = \tfrac{1}{2}\int_{-l}^{l} \frac{\partial t(z)}{\partial H} z \, \mathrm{d}z, \tag{2b}$$

$$\kappa_G^b = \int_{-l}^{l} t(z) z^2 \, \mathrm{d}z, \tag{2c}$$

where $2l$ is the thickness of the bilayer and the origin for the integration is the bilayer midplane, fig. 2. Eqs. (2a) and (2c) were first described by Helfrich [5] and eq. (2b) is due to Szleifer et al. [4]. These integrals are only strictly correct for a flat bilayer and to relate them to measurements of the curvature elastic parameters made on bicontinuous cubic phases one has to imagine the bilayer being pressed flat. In the model we present here we imagine this to be done with little or no net stretching of the bilayer. Another way of putting this is to say that the neutral surface area remains constant. The definition of the neutral surface is somewhat subtle and we leave its description to the following section.

3. Curvature energy in bicontinuous cubic phases

Eq. (1) is quite general; here we require an equation for the curvature elastic energy per unit area which deals specifically with the inverse bicontinuous cubics. In the spirit of Helfrich's treatment of flat bilayers we begin our derivation by modelling the bicontinuous bilayer as an infinitely thin sheet. This sheet will lie on the surface formed by the locus of points defining the average position of the methyl termini of the hydrocarbon chains. The available evidence indicates that the surfaces underlying the bicontinuous cubics are infinite periodic minimal surfaces (IPMS) [13–22], fig. 3. The principal curvatures at all points on such surfaces are equal in magnitude, but opposite in sign. This means that the surfaces have zero mean curvature at all points and Gaussian curvature which is less than or equal to zero.

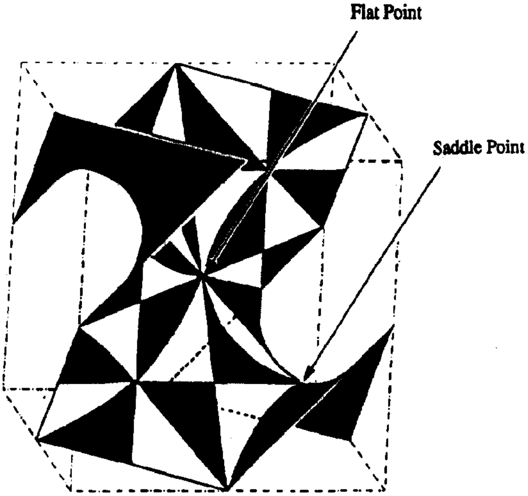

Fig. 3. The D surface (adapted from ref. [23]). The unit cell of the inverse bicontinuous cubic phase of spacegroup Pn3m is based on the D surface shown here. The fundamental surface patches, have been indicated in black and white and we have indicated one of the flat points and the saddle point on one of the six fundamental saddles.

If we model the bilayer of the bicontinuous cubic as an infinitely thin sheet on the IPMS, then the first order expansion in eq. (1) is insufficient to stabilise the phase. This is so, because H is zero by definition and H_0 is zero for a bilayer having identical molecular composition on each side. Hence g_c is simply proportional to K, and K can be made more and more negative simply by shrinking the lattice dimensions, since this increases the magnitude of the principal curvatures. Physically one would expect the phase to stop shrinking when the interfaces are in such close proximity that the repulsive hydration force stabilises the phase. However, many of the bicontinuous cubic phases have water channels which are too large to be stabilized in this way [10,24]. Thus in these cases the system must be stabilized primarily by the curvature elasticity alone, and we must look for higher-order expansions of the curvature elastic energy which lead to stable solutions.

Ljunggren and Eriksson [7] have shown that the lowest-order expansion which makes an IPMS sheet stable to size fluctuations extends to fourth order in curvature

$$g_c = \kappa_G^b K + \kappa_G^{b'} K^2, \qquad (3)$$

where $\kappa_G^{b'}$ is the second-order Gaussian curvature modulus for the bilayer. For the cubics to exist, both the first- and second-order moduli must be positive. Since K varies along the surface of the IPMS, from being zero at the flat points and maximally negative at the saddle points, fig. 3, we must determine the surface averaged value of the curvature elastic energy per unit area, $\langle g_c \rangle$. Using the Gauss–Bonnet theorem to integrate K over the unit cell we obtain

$$\langle g_c \rangle = \kappa_G^b \frac{2\pi\chi}{S_u} + \kappa_G^{b'} \frac{4\pi^2\chi^2 f}{S_u^2}, \qquad (4)$$

where S_u is the surface area of the IPMS within the unit cell, χ is the Euler characteristic of the surface and f denotes $\langle K^2 \rangle / \langle K \rangle^2$ ($\langle \ldots \rangle$ indicates a surface average). The three most common inverse cubic phases (spacegroups Ia3d, Pn3m and Im3m) are based on the G, D and P surfaces respectively, see e.g. ref. [20]. These are related to each other by the Bonnet transformation, which means that f is invariant amongst this set and is equal to 1.2187 [6]. The Euler characteristic within the crystallographic unit cell of each cubic has been calculated by a number of authors and is -8 for G, -2 for D and -4 for P. We can now plot the curvature elastic energy for each of these cubics as a function of the surface area of the unit cell, and as expected we obtain a negative minimum, fig. 4. The equilibrium surface area, S_u^0, and minimum elastic energy can now be found

$$S_u^0 = \frac{-4\pi\chi\kappa_G^{b'} f}{\kappa_G^b}, \qquad (5a)$$

$$\langle g_c^0 \rangle = \frac{-\left(\kappa_G^b\right)^2}{4\kappa_G^{b'} f}. \qquad (5b)$$

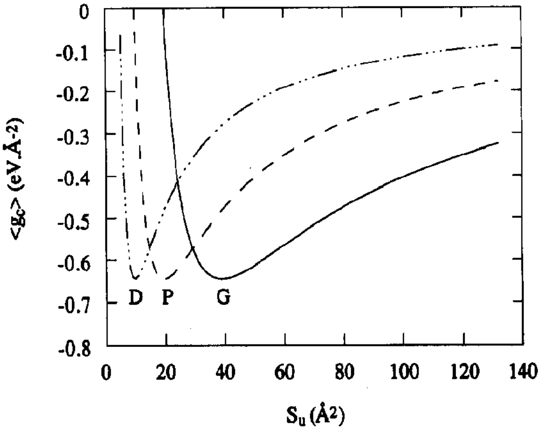

Fig. 4. The curvature elastic energy per unit area $\langle g_c \rangle$ as a function of the IPMS surface area in the unit cell, S_u. We have calculated $\langle g_c \rangle$ for $\kappa_G^b = 1$ eV and $\kappa_G^{b'} = 1$ eV.

We have assumed in our calculations for fig. 4 that the two saddle splay moduli have constant values. Accepting this assumption for the moment, it is clear that the minimum in the curvature elastic energy is exactly the same in each of the three phases. What differentiates the phases is only the way in which they fill space. The equilibrium IPMS surface area is proportional to χ, which means that there is a successive doubling in the area of the underlying IPMS sheet between D, P and G.

Although there is a good deal of information in eq. (4), the model lacks physicality. In particular it does not reflect the fact that in general each monolayer will still be curvature frustrated, although not to the degree it would be if held flat [25]. To reveal this frustration we will now model the system as two monolayers held back to back rather than as a single bilayer. In the same spirit as was previously used to model the bilayer, we will model each monolayer as a two-dimensional sheet positioned a distance $\pm\xi$ from the IPMS sheet which they replace, fig. 5. We can then use the surface metric for the IPMS to map eq. (4) on to one of the new surfaces [8]. Upon doing this we find that this parallel surface possesses mean as well as Gaussian curvature. By equating our mapped version of eq. (4) to eq. (1) we find that to first order the Gaussian moduli for the bilayer can be re-expressed in terms of monolayer parameters

$$\kappa_G^b = 2(\kappa_G - 4\kappa H_0 \xi), \tag{6a}$$

$$\kappa_G^{b'} = 4\kappa\xi^2. \tag{6b}$$

Similar expressions have been derived by a number of other authors [7,26]. The presence of H_0 in the first-order saddle splay modulus reveals the curvature frustration, since H at a distance ξ will in general not be equal to H_0. (It should be noted that we use the convention of negative mean curvature for interfaces with net curvature towards the aqueous phase.)

The distance ξ is set to be the distance to the neutral surface. We define the neutral surface as that *physical* surface, whose area does not vary during hydration. By physical surface we mean a surface associated with a chemical group, for example the average location of the third carbon atom in the chain. The neutral surface as we define it may be located by determining the molecular area at some distance from the underlying IPMS, where the fractional molecular volume between the IPMS and this parallel surface is constant upon hydration. The reason for setting this distance, is that for a given amphiphile at a fixed temperature, κ, κ_G and H_0 are functions of the neutral surface area and nothing else [4]. In other words by studying a hydration sequence at fixed temperature, so long as we can ascertain that there was no bilayer stretching, the elastic parameters will be constant and we may obtain their values.

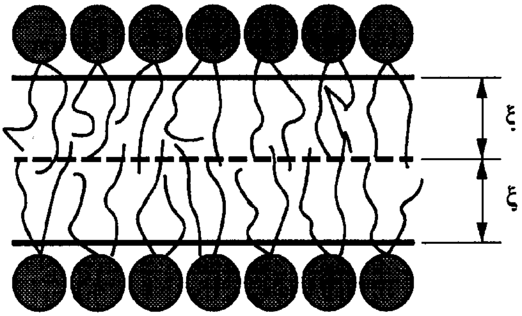

Fig. 5. Modelling physical frustration. The bilayer sheet can be replaced by two monolayer sheets, positioned at the neutral surface, shown here as being at a distance ξ from the bilayer midplane.

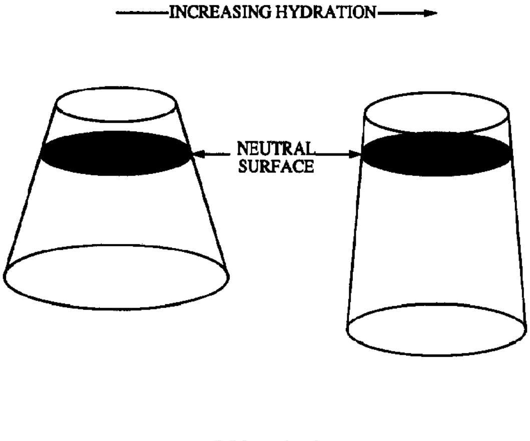

Fig. 6. During hydration the average molecular shape becomes more cylindrical. The mass of sample either side of the neutral surface remains constant, and therefore any change in shape is accompanied by a change in the distance to the neutral surface.

Our definition of the neutral surface is a very restrictive one, and Kozlov and Winterhalter [27] have presented another formalism which allows for cases where there is both bending and stretching of the monolayer in the H_{II} phase. In principle one could use the same formalisms with the bicontinuous cubics, but nobody has yet attempted this; the mathematics appears to be somewhat daunting. Furthermore, we will go on to argue that the regime in which our more restrictive prescription will hold is also the regime in which we may be able to relate the measured elastic moduli to the lateral stress profile.

If we return to our assumption that κ_G^b and $\kappa_G^{b'}$ are constant during hydration we can see from eq. (6) that in fact they are not, unless ξ is a constant. However, in fig. 6 we show that in general ξ is not constant and this means that for the purposes of fitting experimental data and physical understanding it is not sensible to try to use eq. (4). We therefore substitute for κ_G^b and $\kappa_G^{b'}$ in eq. (4) to obtain an equation which explicitly includes the variable ξ,

$$\langle g_c \rangle = \frac{4\pi\chi}{S_u}\left[\kappa_G - 4\kappa H_0 \xi + \frac{4\pi\chi}{S_u} f \kappa \xi^2\right]. \tag{7}$$

Our curvature elastic energy equation is now a function of two variables S_u and ξ. What we will now do is to show that we can express $\langle g_c \rangle$ in terms of only one variable, $I = v/Al$ [28], where v is the amphiphile volume, A is the headgroup cross-sectional area and l is the amphiphile length. To do this we first determine how S_u depends on I.

Using the differential geometric relationships for the IPMS, published by Hyde [8], it is possible to show that the surface area of the IPMS in the unit cell is set by

$$S_u = \tfrac{2}{3}\pi\chi l^2 \left(\frac{3I - 1}{1 - I} \right), \tag{8}$$

which upon substitution into (7) gives

$$\langle g_c \rangle = \frac{6\psi}{l^2} \left[\kappa_G - 4\kappa H_0 \xi + 6\kappa f \psi \left(\frac{\xi}{l} \right)^2 \right], \tag{9}$$

where $\psi = (1 - I)/(3I - 1)$. We now have an expression for $\langle g_c \rangle$ which is a function of I and in addition ξ and l. However, putting our definition of the neutral surface into mathematical terms using some simple geometry and relationships from ref. [8] we obtain the following two expressions for ξ and l which allow us to express $\langle g_c \rangle$ as a function of the molecular shape parameter I alone,

$$\frac{\xi}{l} = \frac{\phi - \sqrt{A_n I l / v}}{\phi - 1}, \tag{10a}$$

$$l = \left(\frac{v_n}{v} 3I(1 - \phi) + \phi^3 \right)^{2/3} \frac{v}{A_n I}. \tag{10b}$$

Here A_n is the cross-sectional area of the neutral surface, v_n/v is the fractional volume of lipid between the IPMS and the neutral surface and $\phi = \sqrt{\left(\tfrac{3}{2}I - \tfrac{1}{2}\right)}$.

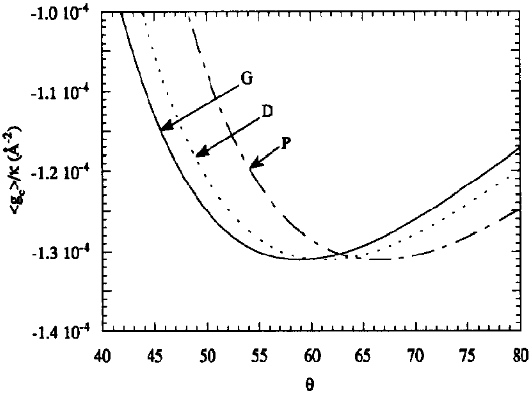

Fig. 7. The normalized curvature elastic energy per unit area $\langle g_c \rangle/\kappa$ as a function of the hydration θ. We have calculated $\langle g_c \rangle/\kappa$ using $\kappa_G/\kappa = 0.048$, $H_0 = -5.1 \times 10^{-3}$ Å^{-1}, $v_n/v = 0.74$ and $A_n = 105.8$ Å^2 for the G, D and P surfaces.

Using $\kappa_G/\kappa = 0.048$, $H_0 = -5.1 \times 10^{-3}$ Å^{-1}, $A_n = 105.8$ Å^2 and $v_n/v = 0.74$ we have calculated $\langle g_c \rangle/\kappa$ as a function of I using eqs. (9) and (10). This has been plotted, fig. 7, for the G, D and P phases as a function of hydration, where the hydration, θ, in moles of water to moles of lipid has been determined using the following relation

$$\theta = \frac{v}{29.9} \left(\sqrt{\frac{\pi\chi(3I - 1)^3}{24\sigma^2 I^2 (1 - I)}} - 1 \right), \tag{11}$$

where 29.9 is the volume of a water molecule in Å^3 and σ is the dimensionless area of the underlying IPMS (σ is equal to 1.919, 2.345, and 3.091 for D, P and G, respectively [29]).

Since $\langle g_c \rangle$ only depends on I as does θ, it is clear that it is the dimensionless area and the Euler characteristic which set the amount of water which each phase can contain at a given value of I. Hence, the model predicts that as a function of hydration the phases should always appear in the sequence G ⇒ D ⇒ P simply because of these space filling properties. As far as we are aware this has so far always proved to be the case. For the same reason all molecular dimensions at the energetic minimum are the same in each phase. The conclusions that were drawn from eqs. (5a) and (5b) therefore do hold true, that is, that the phases are energetically degenerate, and the ratio of the equilibrium surface areas of the underlying IPMS are set by the phase topology alone. It is the details of the shape of the curves away from equilibrium which are different from fig. 4. This difference arises because the monolayer thickness departs from its equilibrium value in dehydrated states. From simple geometrical considerations it can be seen that in materials where the neutral surface lies close to the polar interface l and ξ shrink during dehydration. However, under conditions where the neutral surface lies closer to the underlying IPMS the reverse may be observed. In either case the system is in general physically frustrated both in terms of the amphiphile length and the mean interfacial curvature, the frustration being at a minimum at equilibrium.

4. Measuring curvature energy in bicontinuous cubic phases

In principle it should be possible to measure the curvature elastic parameters by measuring $\langle g_c \rangle$ as a function of hydration and then fitting the data using eqs. (9)–(11). Indeed Chung and Caffrey have shown that such measurements can be made [11] using the osmotic stress technique [30] on the G-surface cubic phase of monoolein in water. Such measurements are difficult to make and the data must be treated with a high degree of care.

It is a prerequisite for the use of the model described here and Turner's model that the position, area and most importantly the existence of the neutral surface is first established. It is clear that the neutral surface as defined for our model, and Turner's will probably not exist at very low hydrations, because here the interfacial curvatures are of the same order as the monolayer thickness. Kozlov and Winterhalter's treatment [27] was specifically developed for such situations. This is unfortunate, because the G surface cubic normally has the greater range of stability with hydration, fig. 7, but is also the most dehydrated cubic phase. It is interesting to note in this respect that Szleifer et al. [4] have found that the chain contribution to κ varies as $A_n^{-7.5}$ (this is for saturated chains). Clearly small variations in neutral surface can make large changes to the elastic parameters.

Given these concerns we have examined preliminary data on 2:1 mol/mol mixtures of lauric acid (LA) and dilauroylphosphatidylcholine (DLPC) in water [31] in which we observe all three cubic phases at varying hydrations, with the aim of attempting to observe where the approximations of our model break down. Our X-ray data for limiting hydration values in each phase are summarised in table 1. We have determined l from the lipid volume fraction, ϕ_l, using

$$\phi_l = 2\sigma\left(\frac{l}{a}\right) + \tfrac{4}{3}\pi\chi\left(\frac{l}{a}\right)^3, \tag{12}$$

where a is the lattice parameter (see e.g. ref. [9]). We have used eq. (11) to determine I, and thence A. The cross-sectional area at the neutral surface

Table 1

Data for the bicontinuous cubic phases of the system lauric acid/dilauroylphosphatidylcholine (2:1 mol/mol) in water

Cubic phase	G	D	P
T (°C)	52 ± 10.03	58 ± 0.03	52 ± 0.03
θ	49 ± 2	55 ± 4	68 ± 2
a (Å)	159 ± 0.5	108 ± 2	143.5 ± 1.5
ϕ_l	0.50 ± 0.01	0.47 ± 0.02	0.42 ± 0.01
l (Å)	13.4 ± 0.3	13.7 ± 0.6	13.3 ± 0.4
I	1.087 ± 0.003	1.079 ± 0.004	1.067 ± 0.003
A (Å^2)	100 ± 2	99 ± 5	103 ± 3
A_n (Å^2)	104 ± 2	102 ± 5	106 ± 3
ξ^0 (Å)	9.9 ± 0.2	10.2 ± 0.5	9.8 ± 0.3
H_n (Å^{-1})	$(-6.4 \pm 0.1) \times 10^{-3}$	$(-5.7 \pm 0.3) \times 10^{-3}$	$(-5.1 \pm 0.1) \times 10^{-3})$

was determined by assuming that the surface was positioned at the third carbon atom along the hydrocarbon chains (this is normally the position of maximum chain incompressibility [4]) and then determining the fractional volume at this position. With a molecular volume for the two fatty acid molecules and one lecithin of 1459 Å^3 we found $v_n/v = 0.740$. We then used eq. (10b) to solve for A_n, and eq. (10a) to determine the distance to the neutral surface at the limiting hydration in each phase, ξ^0. Finally we determined the surface averaged mean curvature defined to the neutral surface, H_n, using the following relation from Hyde [8]:

$$H_n = \frac{2\pi\chi\xi^0}{\sigma a^2}. \tag{13}$$

Our data set is not ideal, because our hydration sequence is, at present, rather sparse. This has meant that the limiting hydrations for each phase are best estimates. This of course has a knock on effect in our determination of all aspects of the molecular geometry. The errors we report attempt to reflect this. A further effect of the paucity of our data set has been that in the region of the isotherm where all the evidence indicates we should find a Pn3m bicontinuous cubic phase (D surface) we have, as yet, no data. This has meant that we have had to use data for Pn3m on an isotherm at 58°C, which is 6°C greater than that at which our data on the Ia3d (G surface) and Im3m (P surface) cubic phases were obtained. Clearly a rise of 6° will change the values of all the curvature elastic parameters, but we should not expect the change to be too great.

We know that as long as the neutral surface remains constant that at equilibrium the molecular geometry in each phase will be identical. Within experimental error the neutral surface area appears to be the same in each phase. Similarly A, l, and ξ^0 do not appear to vary. However, this is deceptive, since the errors in these measurements are larger than the changes which are occuring. These changes can be confirmed by noting that I and H_n should also have the same value in each phase at equilibrium, but it is clear that this is not the case. If we are to observe changes in neutral surface area directly, the precision with which determinations of lipid volume fraction and lattice parameter are made will have to be improved by an order of magnitude or more (see ref. [9] also).

Notwithstanding these problems we have made an estimate of κ_G/κ and H_0 from the data on the P cubic phase at equilibrium. We do this by using eq. (5a) and (6) to obtain

$$\frac{\kappa_G}{\kappa} - 4H_0\xi^0 = -\frac{8\pi\chi f(\xi^0)^2}{\sigma a^2}. \tag{14}$$

The spontaneous mean curvature should have a value very close to the actual mean curvature [7] so we set $H_0 = H_n$, and this gives us $\kappa_G/\kappa = 0.048$. The reader will recognise that these are the values used to plot $\langle g_c \rangle/\kappa$ as a function of θ in fig. 7. Recalling that a typical value for κc in phospholipids is ≈ 1 eV we calculate the curvature elastic energy per LA/DLPC complex to be 8.5 meV ($kT = 25$ meV). Given the range of assumptions we have made to get to this estimate, this does not seem unreasonable.

The value of κ_G/κ is positive, and rather small. This is quite different from the values calculated for didodecyl-β-D-glucopyranosyl-*rac*-glycerol [9] where κ_G/κ is negative and approximately six times the magnitude of the value reported here. It was stated earlier that one of the conditions for cubic phase stability was that $\kappa_G^b > 0$. Referring back to eq. (6a) it is clear that this condition can still hold even if κ_G is negative (remember H_0 is negative). In other words cubic phases may be formed even though it is energetically unfavourable to bend the monolayer into a saddle surface. In such cases the system is being driven into a bicontinuous cubic phase simply because of a strong desire for a mean interfacial curvature intermediate between those of the L_α and H_{II} phases. This would appear to be the case for the glucolipid. However, in the fatty acid/lecithin mixture it appears that there is in fact a positive if small desire for Gaussian curvature.

Turner et al. [9] state that this will not occur since a positive value of the saddle splay modulus would cause the phase to increase its saddle curvature ad infinitum. According to our model this is not the case, since Ljunggren and Eriksson [7] explicitly include a stabilizing term in the curvature elastic energy (eq. (3)). In fact this is, we believe, also implicit in Turner's model [9] and this is borne out by Chung and Caffrey's study of monoolein [11] where Turner's eqs. have been used and a large and positive value for κ_G is found. In this respect we feel the more explicit derivation and nature of the expressions reported here are advantageous.

Unfortunately the differences in the model reported here and in ref. [9] appear to be deeper than the way in which they have been derived and presented. We have taken the reported equilibrium values from [9] of $a = 91.5$ Å, $H_0 = -\frac{1}{36}$ Å^{-1} and $\xi^0 = 16.5$ Å (defined to the headgroup at 45°C) in the D surface cubic and calculated κ_G/κ. Using (14) we obtain a value of -0.795 compared to their calculations which give a value of -0.454. So although both models agree qualitatively in making the modulus negative, there is a significant quantitative discrepancy between the two models. Where this difference arises in the models is at present not known.

5. Determining the lateral stress experimentally

As we have already stated it is our long term aim to use measurements of κ_G, κ and H_0 in order to determine the form of the lateral stress profile. So, in a rather more speculative vein than hitherto, we now go on to see how determinations of κ_G, κ and H_0 might be used to determine the lateral stress profile.

The first point that we should recall is that the lateral stress integral eqs. (2a)–(2c) hold true for flat films [3,4]. This means that when we determine the lateral stress from our bicontinuous cubic phase data we imagine that the bilayer has been flattened out, and that this was done at constant neutral surface area. The reason for doing this is not merely to simplify the computations. By determining $t(z)$ for a flattened monolayer, we will have calculated a function which varies smoothly with thermodynamic variables, but will be used to describe the discontinuous behaviour of a phase transition.

Since we are measuring monolayer quantities at the neutral surface we have to transform the stress integrals to make them consistent with the relationships in eqs. (6a) and (6b)

$$\kappa H_0 = -\tfrac{1}{2}\int_0^{l'} t(z)(z-\xi')\,\mathrm{d}z, \tag{15a}$$

$$\kappa = \tfrac{1}{2}\int_0^{l'} \frac{\partial t(z)}{\partial H}(z-\xi')\,\mathrm{d}z, \tag{15b}$$

$$\kappa_G = \int_0^{l'} t(z)(z-\xi')^2\,\mathrm{d}z. \tag{15c}$$

The new values of l and ξ (l' and ξ') arise because of the flattening of the monolayer. These values can be very easily calculated by using eq. (10) and setting $I = 1$, i.e. the flat state. The position $z = 0$ is at the terminal methyl group on the hydrocarbon chains and the first and second moments of the stress are calculated about the fulcrum formed by the neutral surface, hence the term $z - \xi'$.

As we have already mentioned, the stress profile in the chain region can be modelled [4]. This leaves the stress in the interfacial and headgroup regions to be determined. We propose that these might be modelled in some simple way, for example as two Gaussians. This would leave us six parameters to be determined, the mean position, maximum stress and the full width at half maximum of the headgroup and interfacial components. The integrals in (15) give us only three independent equations, but we also know that the total integrated stress is zero and a further two constraints can be applied, first that the total width of the flat monolayer must not exceed l' and second that the neutral surface (or fulcrum) should be located at ξ'.

Clearly the constraints and modelling will never give rise to anything other than a rather crude approximation to the actual stress profile. However, before we even get to the stage of trying to make this determination we should recall that there are important restrictions on the primary X-ray measurements which can be used.

The most important restrictions are that all the transverse energy terms should be negligible, there should be no net bilayer stretching during the measurements, and that the polar–apolar interface should be parallel to the parent IPMS. These conditions are only likely to be met where the radius of curvature at the polar–apolar interface is greater than the monolayer thickness. The critical question is of course how much greater does it have to be?

A quick way of finding out whether a bicontinuous cubic is sufficiently large, which does not involve the calculation of the molecular geometry, relies on eq. (5a). This states that when bicontinuous cubic phases are stabilized by the curvature elastic energy alone, their relative equilibrium areas are topologically fixed. In phase diagrams where we have two or more cubics on an isotherm we can use measurements of the equilibrium lattice parameters to see whether the curvature elastic approximation described here will hold. Where it does the ratio of equilibrium lattice parameters should be $a_D : a_P : a_G = 1:1.28:1.58$.

If we look at the case of monoolein we have G- and D-surface cubic phases and according to [11] $a_D : a_G \approx 1:1.50$ at 25°C, the D phase having an equilibrium lattice parameter of ≈ 100 Å and the G phase 150 Å. Clearly the curvature elastic approximation described here will not hold at these dimensions relative to the lipid length. This is confirmed in didodecyl-β-D-glucopyranosyl-*rac*-glycerol [9] which also has G- and D-surface cubic phases. The largest lattice parameters are achieved at 35°C and here $a_D : a_G = 1:1.50$, with $a_D = 97.9$ Å and $a_G = 146.4$ Å. For the 2:1 (mol:mol) mixture of lauric acid and dilauroylphosphatidylcholine we get $a_D : a_P = 1:1.33$, table 1. This is getting closer to the theoretical prediction of 1.28, and this is occurring, as we would expect, as our lattice dimensions increase with respect to the lipid length. Of course the question now arises as to whether there are any systems which are sufficiently large so that we can apply the curvature elastic model.

The largest cubic phases we have identified [24] are in a mixture of monoolein, dioleoylphosphatidylethanolamine and dioleoylphosphatidylcholine (0.58:0.09:0.33 molar ratios). We find a coexistence of the D and P phases at room temperature in excess water which lasts for at least a few hours after which the P phase disappears. The ratio in the measured lattice parameters is $a_D : a_P = 1.28 \pm 0.02$, in agreement with the theory. Here a_P is measured to be 270 ± 3 Å. Using an estimate of the distance to the neutral surface of 11 Å we find $H_n = -1/618$ Å^{-1}, so with $H_n^{-1} \approx 50\xi$ we should obtain results which agree with the theory. At what stage the model no longer works has not yet been ascertained.

6. Conclusions

It would appear that where bicontinuous cubic phases are sufficiently dilated the mesophase is stabilised almost entirely by the curvature elastic energy. It is possible to ascertain that a system is in this regime by measuring the ratios of equilibrium lattice parameters between any fully hydrated swollen cubic phases which occur at fixed temperature. By applying the curvature elastic model to such systems it should be possible to extract values for the monolayer elastic constants which are directly related to integrals of the lateral stress. Furthermore the elastic moduli measured in this way should be directly comparable with measurements using macroscopic techniques [32].

The model has a number of approximations which may cause difficulties in the interpretation of data at high interfacial curvature. We have discussed at length the problems which may arise due to monolayer stretching in this regime, but a difficulty also arises by modelling the interface as a surface parallel to the underlying IPMS. Because the Gaussian curvature is a function of position on the IPMS the mean curvature at the interface is also a function of position. This has the effect of creating a non-uniform interfacial tension. The problem is once again minimised when the curvature is not too great with respect to the molecular length (see ref. [25] for more details). We also note that this model does not incorporate any contribution from lattice fluctuations in the elastic energy, and that this may have significant consequences as the lattice parameter becomes large [33].

Acknowledgement

This work was supported by grants from the SERC (grant Nos. GR/F44052, GR/H10672 and GR/H69229), and the Royal Society, who supported RHT in the form of a University Research Fellowship. We also wish to thank Jan Christer Eriksson for his help in explaining the mysteries of curvature energy and Jean Charvolin, Alan Mackay, Jean-François Sadoc and Humberto Terrones for their help in understanding the geometry of minimal surfaces.

References

1 J.M. Seddon and R.H. Templer, Phil. Trans. Roy. Soc. London A 344 (1993) 377.
2 J.M. Seddon, Biochim. Biophys. Acta 1031 (1990) 1.
3 W. Helfrich, in: Physics of defects, eds. R. Balian et al. (North-Holland, Amsterdam, 1981) p.715.
4 I. Szleifer, D. Kramer, A. Ben-Shaul, W.M. Gelbart and S.A. Safran, J. Chem. Phys. 92 (1990) 6800.
5 W. Helfrich, Z. Naturforsch. 28c (1973) 693.
6 W. Helfrich and H. Rennschuh, J. Phys. (Paris) 51 (C7) (1990) 189.
7 S. Ljunggren and J.C. Eriksson, Langmuir 8 (1992) 1300.
8 S.T. Hyde, J. Phys. Chem. 93 (1989) 1458.
9 D.C. Turner, Z.-G. Wang, S.M. Gruner, D.A. Mannock and R.N. McElhaney, J. Phys. II France 2 (1992) 2039.
10 P. Ström and D.M. Anderson, Langmuir 8 (1992) 691.
11 H. Chung and M. Caffrey, Nature, submitted for publication.
12 J.F. Sadoc and J. Charvolin, J. Phys. (Paris) 47 (1986) 683.
13 L.E. Scriven, Nature 263 (1976) 123.
14 L.E. Scriven, in: Micellization, solubilization and microemulsions, Vol. 2, ed. K.L. Mittal 2 (Plenum Press, New York, 1977) p. 877.
15 W. Longley and T.J. McIntosh, Nature 303 (1983) 612.
16 S.T. Hyde, S. Andersson, B. Ericsson and K. Larsson, Z. Krystallogr. 168 (1984) 213.
17 J. Charvolin, J. Phys. (Paris) 51 (C7) (1985) 35.
18 A.L. Mackay, Nature 314 (1985) 604.
19 W. Helfrich and W. Harbich, in: Physics of amphiphilic layers, eds. J. Meunier, D. Langevin and N. Boccara (Springer, Berlin, 1987) p. 58.
20 S. Andersson, S.T. Hyde, K. Larsson and S. Lidin, Chem. Rev. 88 (1988) 221.
21 P. Mariani, V. Luzzati and H. Delacroix, J. Mol. Biol. 204 (1988) 165.
22 E. Dubois Violette and B. Pansu, eds., International workshop on geometry and interfaces, J. Phys. (France) 51 (C7) (1990).
23 A.L. Mackay and J. Klinowski, Comp. Math. Appl. 12B (1986) 803.
24 R.H. Templer, K.H. Madan, N.A. Warrender and J.M. Seddon, in: The structure and conformation of amphiphilic membranes, eds. R. Lipowsky, D. Richter and K. Kremer (Springer, Berlin, 1992) p. 262.
25 D.M. Anderson, S.M. Gruner and S. Leibler, Proc. Natl. Acad. Sci. US 85 (1988) 5364.
26 G. Porte, J. Appell, P. Bassereau and J. Marignan, J. Phys. (Paris) 50 (1989) 1335.
27 M.M. Kozlov and M. Winterhalter, J. Phys. II (Paris) 1 (1991) 1077.
28 J.N. Israelachvili, D.J. Mitchell and B.N. Ninham, Quart. Rev. Biophys. 13 (1980) 121.
29 D.M. Anderson, H. Wennerstrom and U. Olsson, J. Phys. Chem 93 (1989) 4243.
30 R.P. Rand, N. Fuller, S.M. Gruner and V.A. Parsegian, Biochemistry 29 (1990) 76.
31 N.A. Warrender, Ph.D. Thesis, Imperial College (1992).
32 E. Evans and D. Needham, in: Physics of amphiphilic layers, eds. J. Meunier, D. Langevin and N. Boccara (Springer, Berlin, 1987) p. 38.
33 R. Bruinsma, J. Phys. II (Paris) 2 (1992) 425.